# INVESTIGATING DESIGN PARAMETER EFFECTS ON THE CURVATURE OF COMPOSITE SOFT ACTUATORS BY AUTOMATED NUMERICAL SIMULATION

# Hiep Xuan Trinh<sup>1</sup>,\*, Van Binh Phung<sup>2</sup>

WITH PYTHON INTEGRATION

<sup>1</sup>Faculty of Mechanical Engineering, Le Quy Don Technical University, Hanoi, Vietnam <sup>2</sup>Faculty of Aerospace Engineering, Le Quy Don Technical University, Hanoi, Vietnam \*E-mail: hieptx@mta.edu.vn

Received: 24 September 2024 / Revised: 31 December 2024 / Accepted: 03 January 2025 Published online: 21 January 2025

Abstract. In the realm of soft robotics, investigating the effect of design parameters on the deformation of complex structures like soft composite actuators is a challenging task. Existing mathematical models often rely on limiting assumptions, while traditional simulation approaches demand substantial computational time and resources, hindering concurrent investigations of multiple design parameters. To address these issues, this paper introduces a new technique to expedite the deformation simulation of composite soft actuators. This automation program enables automatic modification of input parameters while preserving critical properties, constraints, and boundary conditions, resulting in a significant reduction in simulation time. Compared to traditional methods requiring approximately 60 minutes for a single task, our technique achieves the same in merely 10 minutes. The developed program is applied to analyze the impact of design parameters on the curvature of composite soft actuators, leading to the identification of optimal parameters. Through experimental verification, the reliability and efficiency of our technique are demonstrated, showing simulation results with less than a 10% error when compared to physical experiments. The proposed approach enables swift investigation of design parameter influence, facilitating the identification of optimal soft robotic structures for specific objectives. As a result, it has the potential to become a promising tool for advancing soft robotics design and analysis.

*Keywords*: soft composite actuator, numerical simulation, Python integration, soft robotic structure.

### 1. INTRODUCTION

Soft robotics is currently a highly promising field of research, offering distinct advantages over traditional robots. These soft robots are capable of safe interaction with humans and possess the ability to autonomously adjust their physical configurations to effectively adapt to various environments [1, 2]. The scope of soft robotics research encompasses diverse areas, including soft actuators, soft sensors, and locomotion [3–5]. Among these, the study of designing and fabricating soft actuators has achieved remarkable outcomes. By exploiting the deformable properties of soft materials, these actuators demonstrate enhanced flexibility compared to their traditional counterparts [6,7]. They can operate without limitations in terms of degrees of freedom and workspace, and exhibit the capacity to adapt to a wide range of deformations and shapes. Consequently, soft actuators find versatile applications in various fields, such as medicine [8], assisting individuals with disabilities [9, 10], and enabling effective manipulation through robot hands or soft grippers [11, 12]. The operation of soft actuators primarily relies on two main activation principles: pneumatic and hydraulic systems, which offer benefits like rapid response and flexibility [13, 14]. When subjected to pneumatic or hydraulic pressure, these soft actuators undergo deformation, enabling various manipulation shapes such as curvature, elongation, compression, and torsion. Numerous soft actuators have been proposed based on these principles, leveraging the advantages they offer. For instance, in [15], the authors presented the development of a soft pneumatic actuator, by using 3D printing technology. This actuator has a high-force soft exoskeleton that can provide up to 100 N of tip force and aims to assist the user in elbow flexion. In [16], the three water hydraulic soft actuators that are simple and suitable for small autonomous underwater systems were introduced. The popular soft actuators are normally composed of serial chambers, etc., but such structures lead to the possibility of easy detection and failure of the actuator. Thus, to address the issues, a promising design direction involves the development of composite soft actuators. These actuators are constructed using multiple layers of soft materials, with reinforced fibers embedded between these layers. By adopting this approach, researchers aim to enhance the durability and performance of soft actuators. Numerous studies have been conducted, resulting in the successful fabrication and application of these composite soft actuators across diverse fields [17–19]. But, the modeling of deformation and operation for complex structures like soft composite actuators poses a significant challenge. Especially, one crucial aspect is studying the impact of design parameters to optimize their performance. Numerous research endeavors have focused on developing mathematical models to describe the performance of these actuators [20–22]. However, most of these models are proposed for specific designs, relying on assumptions and simplifications regarding material properties and geometric configurations. Consequently, these models cannot be readily applied to a wide range of actuators with different design parameters. Another approach to tackle this challenge is to employ numerical simulations utilizing simulation software [23, 24]. Nonetheless, this method is time-consuming and demands significant computational resources, particularly due to the nonlinear nature of soft materials and the complexity of large deformations. Simulating the deformation of composite soft actuators with numerous design parameters to investigate their influences and determine suitable design parameters for specific purposes can be time-consuming. To overcome these obstacles, this paper proposes a solution that involves the integration of a Python program into the numerical software Abaqus. This approach aims to automate the deformation simulation of composite soft actuators. By employing Python scripting, the simulation can automatically update the new design parameters while the unchanged factors of material properties, constraints, and boundary conditions that remain are preserved throughout the process, resulting in mitigating the computational time and resource requirements. The simulation process can be automatic, enabling efficient exploration of various design parameter combinations and facilitating the identification of optimal design parameters for specific design purposes.

The contributions of this paper are summarized in the following key points:

- 1) The study introduces a Python integration into the Abaqus numerical simulation software, enabling full automation of the simulation process. This advancement reduces computation time significantly, from 60 minutes to just 10 minutes, particularly when analyzing multiple design parameters. It effectively addresses the primary challenges of lengthy computation times often encountered in simulating complex structures, as well as the constraints imposed by the simplifying assumptions of theoretical models.
- 2) This study conducts a detailed analysis of various design parameters, including layer thickness, reinforced fiber diameter, and twist angle, examining their impact on the deformation of soft composite actuators. Through this analysis, an optimal set of design parameters for the actuator is identified.
- 3) The automated parameter investigation method proposed in this study is not limited to soft actuators but also has potential for application in the design optimization of other composite structures within the field of soft robotics.

The rest of the paper is organized as follows: Section 2 provides a brief mechanical design of the composite soft actuator and details the numerical method, which incorporates a Python program for seamless integration, then the numerical analysis is performed with various case parameters to investigate the actuator's deformation. In Section 3, the experiment is conducted to verify the effectiveness of the proposed method. The final section presents a comprehensive discussion and conclusion.

### 2. METHODS

In this section, we introduce a brief mechanical design of the composite soft actuator and the numerical method with integration of Python script to investigate the influence of the design parameters on the deformation of this actuator.

# 2.1. Mechanical design of the composite soft actuator

In our study, we investigated the influence of various parameters on a popular design of pneumatic composite soft actuators [20, 21, 25, 26]. This design consists of four main components, namely the main body layer, neutral layer, reinforcement layer, and cladding layer (Fig. 1).

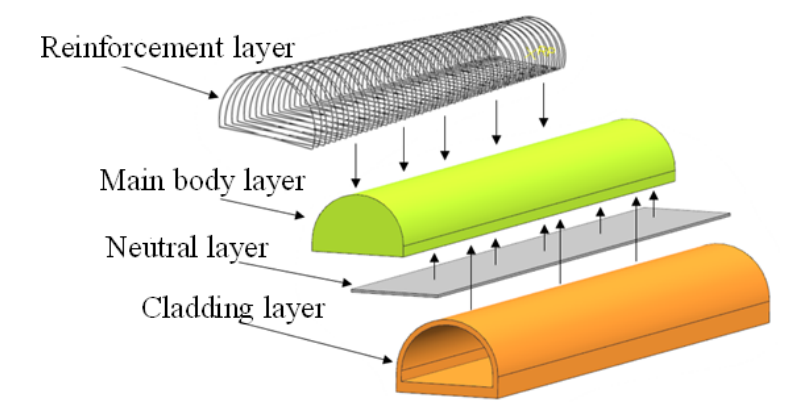


Fig. 1. The structure design of the composite soft actuator

The main body layer has a semicircular cross-section and contains an air cavity, which is sealed at both ends. One end is sealed, while the other is connected to a compressed air tube. The neutral layer, positioned at the bottom of the main body layer, is properly designed to ensure the desired deformation of the actuator when inflated. It can be divided into segments of varying lengths, allowing the actuator to deform differently in each segment to suit its intended purpose. Reinforced fibers are wound around the main body and cladding to increase the actuator's rigidity and limit swelling deformation, thereby enhancing curved deformation. The fibers are wound with different twist angles in various segments to achieve different deformations, such as bending and twisting of the actuator.

In our investigation, we focused on several design parameters to assess their influence on the actuator's deformation. These parameters include the thickness of the main body and cladding layer, the thickness and length of the segments in the neutral layer, and the diameter and torsion angle of the reinforced fibers. By studying the effects of

these parameters, we aimed to optimize the actuator's performance and tailor it to specific design requirements. To achieve this objective, the deformation of the composite soft actuator is simulated using Abaqus/CAE software. This software integrates a built-in calculation program in the form of a Python 2.7.3 Script file. The design parameters are automatically adjusted within the script file to facilitate the calculation process. By modifying these parameters within the script file, different variations of the actuator design can be simulated and analyzed to observe their effects on the actuator's deformation. This automated approach streamlines the simulation process and enables efficient exploration of various design configurations.

# 2.2. Material models and governing equations

A hyperelastic material model relies upon the definition of the strain-energy function, which assumes different forms according to the material or class of materials considered. This function is obtained from symmetry, thermodynamic and energetic considerations. If the material is isotropic, the strain-energy functions *W* depend upon the strain invariant.

$$W_{isotropic} = W(I_1, I_2, I_3), \tag{1}$$

where 
$$I_1 = \sum_{i=1}^{3} \lambda_i^2$$
,  $I_2 = \sum_{i=1}^{3} \lambda_i^2 \lambda_j^2$ ,  $i \neq j$ ,  $I_3 = \prod_{i=1}^{3} \lambda_i^2$ , and  $\lambda_1, \lambda_2, \lambda_3$  are the principal stretches.

There are several forms of strain energy function W for hyperelastic material, such as the Mooney–Rivlin model, the Ogden model, the Arruda–Boyce model, the Neo–Hookean model, and the Gent model [27]. In this paper, the Yeoh model for incompressible materials is used to model RTV 230 Silicone, which is used for the main body layer and cladding layer of a soft actuator. The original model proposed by Yeoh had a cubic form with only  $I_1$  dependence and is applicable to purely incompressible materials. The strain energy density of this model is written as

$$W = \sum_{i=1}^{3} \left[ C_{i0} (I_1 - 3)^i + \frac{1}{D_i} (J - 1)^{2i} \right], \tag{2}$$

where  $C_{i0}$ ,  $D_i$ , J are the material constants and  $I_1 = \lambda_1^2 + \lambda_2^2 + \lambda_3^2$  is the invariant of the Green deformation tensor.

For an incompressible hyperelastic material (J = 1), then the strain energy density of Yeoh is simplified as

$$W = C_{10}(I_1 - 3)^1 + C_{20}(I_1 - 3)^2 + C_{30}(I_1 - 3)^3.$$
 (3)

For the hyperelastic material, the deformation's governing differential equations of the physical body  $\Omega$  can be expressed as

$$\nabla \odot \sigma(t) + b(t) = 0, \tag{4}$$

where  $\sigma$  is the Cauchy stress, b is the body force, and t is the time.  $\nabla$  is the Hamiltonian operator and  $\odot$  denotes the dot product. The governing equations are solved within boundary conditions, including the displacement boundary  $\Gamma_u$  and the traction boundary  $\Gamma_p$  as below:

- On 
$$\Gamma_u$$

$$u(t) = \bar{u}(t), \tag{5}$$

- On 
$$\Gamma_p$$

$$\sigma(t) \odot n = p(t), \tag{6}$$

where  $\bar{u}$  and p are the prescribed displacement and traction, respectively. The Cauchy stress  $\sigma$  is determined by the stress-strain relation. That depends on the hyperelastic material model. For the Yeoh hyperelastic model, the stress-strain formula can be expressed as

$$\sigma_i = \lambda_i \frac{\partial W}{\partial \lambda_i},\tag{7}$$

with strain-energy functions *W* is determined as in Eq. (3).

In this study, the governing equations are automatically solved by Abaqus's computational kernel using the finite element method (FEM). The input parameters, such as material properties, boundary conditions, and calculation loops, are encoded in the integrated Python program.

### 2.3. Numerical simulation method

The automation of design calculations on finite element method (FEM) software, such as Abaqus, typically involves three main stages: pre-processing, processing, and post-processing. These stages are illustrated in Fig. 2(a). The pre-processing stage entails several steps, including the creation of a geometric model and the development of a finite element computational model. During this stage, the geometry of the design is constructed, and appropriate finite elements are defined to discretize the model. The processing phase involves the interpretation of input data and the actual computation of results. Input data may include material properties, boundary conditions, and loading conditions. The software performs calculations based on these inputs to determine the desired results, such as stress, strain, or displacement. Finally, the post-processing stage focuses on accessing, reading, writing, sorting, and visualizing the computed results. This stage allows for the analysis and interpretation of the obtained data. In the

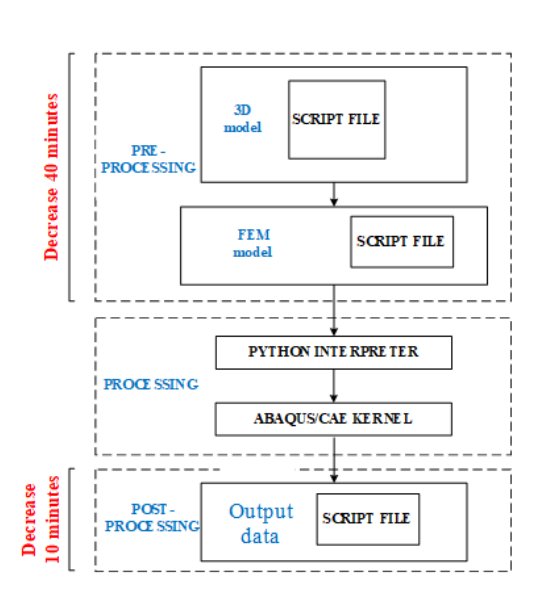
traditional simulation approach, any modification to a parameter requires the entire simulation process to be repeated, leading to significant computational time, particularly when multiple design parameters need to be adjusted.

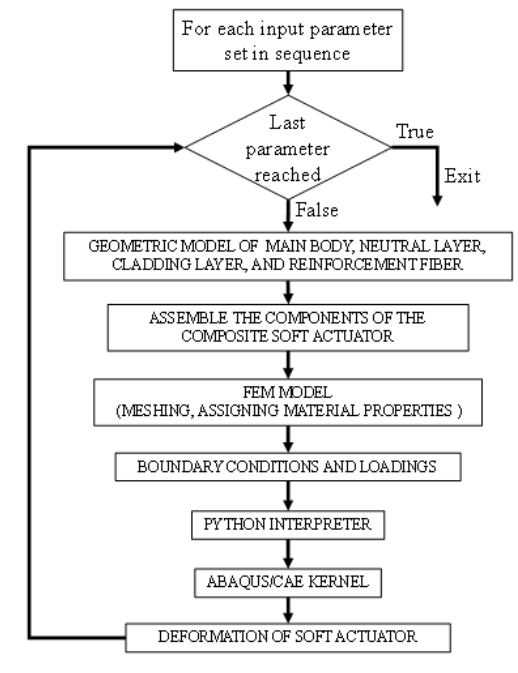
In our technique, an auto-computing program directly integrates with the calculation stage of traditional simulations (as depicted in Fig. 2). Specifically, during the preprocessing stage, a calculation program is established to enable parameterization of the soft actuator model and provide a comprehensive description of the FEM model's characteristics. This includes specifying the element type, size, material properties, boundary conditions, applied pressure, and the type of analysis to be conducted. The calculation program allows for the automatic calculation of new design options by updating a new set of parameters. It ensures that properties, constraints, and boundary conditions that remain unchanged are preserved throughout the process. The Script file is then directly linked to the Abaqus/CAE compute kernel through the Python interpreter, enabling seamless and automatic computation. In the post-processing stage, the Script file is programmed to automatically read, organize, and export the results in a tabular format, facilitating the analysis process. This new approach ensures a continuous and uninterrupted calculation process, performed entirely automatically. Additionally, the pre-processing and post-processing times are significantly reduced. As a result, the total simulation calculation time for a design alternative is reduced to approximately 10 minutes, in comparison to about 60 minutes for the traditional simulation approach.

The automatic program is constructed following the outlined steps:

Step 1: Building a 3D rendering program for the soft actuator (Fig. 3): The calculation program automatically generates the 3D models of the composite soft actuator components within the Abaqus software.

Step 2: Developing a material assignment program: Once the 3D models are created, the program proceeds to automatically assign the appropriate material properties to each component. In this case, the RTV 230 Silicone material is used for the main body and the outer cover of the soft finger. It is characterized as a super elastic, isotropic material with a density of 1140 kg/m<sup>3</sup>. The material properties are assigned based on the Yeoh model using coefficients  $C_1 = 0.11596$ ,  $C_2 = 0.0168$ , and  $C_3 = -0.000319$ . The neutral layer employs fabric materials with the following basic parameters: density of 750 kg/m<sup>3</sup>, elastic modulus of 6500 MPa, and Poisson's coefficient of 0.2. The reinforcement consists of a fabric fiber with a density of 1201 kg/m<sup>3</sup>, modulus of elasticity E = 31076 MPa, and Poisson's coefficient of 0.36.





- (a) The schematic of automation design with Python script integration
- (b) The flowchart of a calculated program

Fig. 2. The schematic of approach method for automated numerical simulation with Python integration

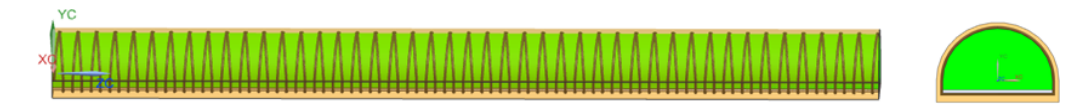


Fig. 3. Completed structure of the composite soft actuator

Step 3: Developing a program to assemble the components of the composite soft actuator: After creating the individual components and assigning the appropriate materials, the program proceeds to automatically assemble the components, ensuring they are combined to form a complete structure as depicted in Fig. 4.

In this step, the calculation program is designed to automatically define the boundary conditions and establish the compressed air pressure for the simulation. The soft actuator is fixed at one end using a clamping mechanism, while the other end is left free, resembling a cantilever beam configuration. The airflow inside the gripper is represented by a uniformly distributed pressure applied to all surfaces within the actuator's air duct (as depicted in Fig. 5). The pressure values are varied within a range from 0 to 250 kPa

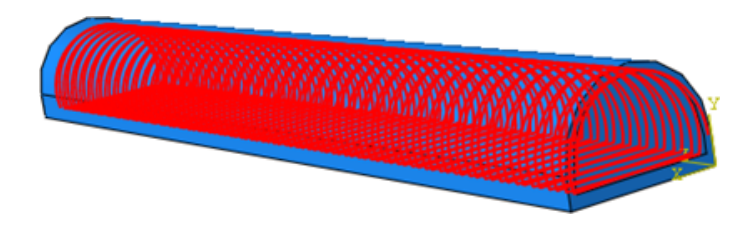


Fig. 4. The completed assembly of the composite soft actuator

to investigate the different curvatures of the actuator. Additionally, gravitational acceleration is considered in the simulation to account for the effect of gravity on the actuator's behavior.

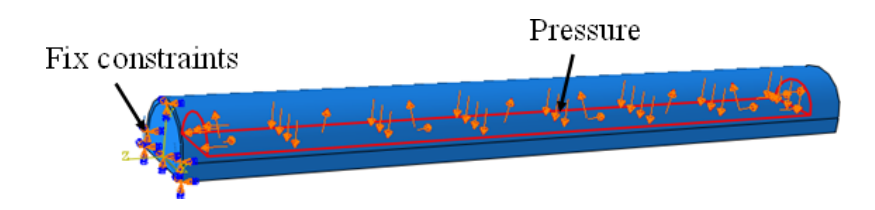


Fig. 5. The boundary condition and external force setup of the composite soft actuator

Step 5: Developing a program to create contact interaction between reinforcement fibers and the main body's wall: In this step, the calculation program is designed to establish the contact interaction between the wall of the main body layer and the reinforcing fibers. This connection is represented using a "tie constraint", which simulates the bonding between the two surfaces without allowing relative motion or separation.

Step 6: Develop an element meshing program: The main body and cladding layer are modeled using uniform solid elements. To accurately represent the complex shape of the soft actuator, a tetrahedral 3D mesh pattern is employed. However, due to the size and complexity of the actuator, the size of each tetrahedral element should not exceed 7 mm. Given the superplastic nature of silicon material, the appropriate element type to be used is the second-order nonlinear element, which can capture the material's nonlinear behavior effectively. The neutral layer, on the other hand, is modeled as a uniform shell element, considering its characteristics and function within the actuator. For the fiber reinforcement, the end of the model is represented using beam elements, which provide a suitable approximation for this specific component. The element size for the reinforcement should be divided into segments no larger than 1.5 mm, ensuring an accurate representation of its behavior.

Step 7: Building the program to create and run the analysis (Create job): In the final step, the calculation program is designed to create the analysis process and input the established data for analysis. The details of the Python script and the numerical simulation can be found in the supplementary material and video link<sup>1</sup>.

# 2.4. Numerical analysis

# **2.4.1.** Numerical investigation setup

The actuator's deformations depend on its design parameters, including the thickness of the main body layer, neutral layer, cladding layer, and the diameter and torsion angle of the reinforced fibers. To examine the impact of each parameter on the actuator's deformation, a systematic approach was adopted. Whereas, each parameter was individually varied while keeping the other parameters constant. All of the case studies were analysed with the length of the soft actuator at 140 mm, keeping the activation pressure constant with the value of 250 kPa. The remaining parameters in specific cases are as follows:

Case of study 1: The thickness of the cladding layer is varied. First, we investigated the curvature of the actuator while varying the thickness of the cladding layer, while the other design parameters are: The thickness of the main body and neutral layer is 2 mm and 0.4 mm, respectively. The twist angle of the reinforcement fiber is  $4^{\circ}$ . The cladding layer thickness is varied from 0 mm to 2.5 mm to observe its impact on the curvature of the soft finger.

Case of study 2: The thickness of the main body changes. In this particular investigation, the main body thickness gradually increases from 0.5 mm to 3 mm while the thickness of the cladding layer and neutral layer is 1 mm and 0.4 mm, and the wire twist angle of the reinforcement fiber is  $4^{\circ}$ .

Case of study 3: The thickness of the neutral layer is varied. In this investigation, the thickness of the neutral layer is varied from 0.1 mm to 0.5 mm. And the thickness of the main body layer and cladding layer is 2 mm and 0.4 mm, respectively. The wire twist angle of the reinforcement fiber is  $4^{\circ}$ .

Case of study 4: The diameter of the reinforcement fiber changes. In this case, the thickness of the layers is kept unchanged compared to the above case studies, while the twist angle of the reinforcement fiber is  $4^{\circ}$  and its diameter is varied from 0.2 mm to 0.7 mm.

Case of study 5: The twist angle of the reinforcement fiber changes. The soft actuator investigated in this case has the following specifications: The thickness of the main body,

<sup>&</sup>lt;sup>1</sup>Abaqus Python scripting for soft actuator - YouTube.

neutral layer, and cladding layer is 2 mm, 0.4 mm, and 1 mm, respectively. The wire fiber is symmetrically twisted around the main body, with one side twisted to the right and the other side twisted to the left. The twist angle ranges from  $3^{\circ}$  to  $15^{\circ}$ .

# **2.4.2.** Numerical results

The curvature of the actuator's results, simulated in the above case studies are presented in Fig. 6 to Fig. 10.

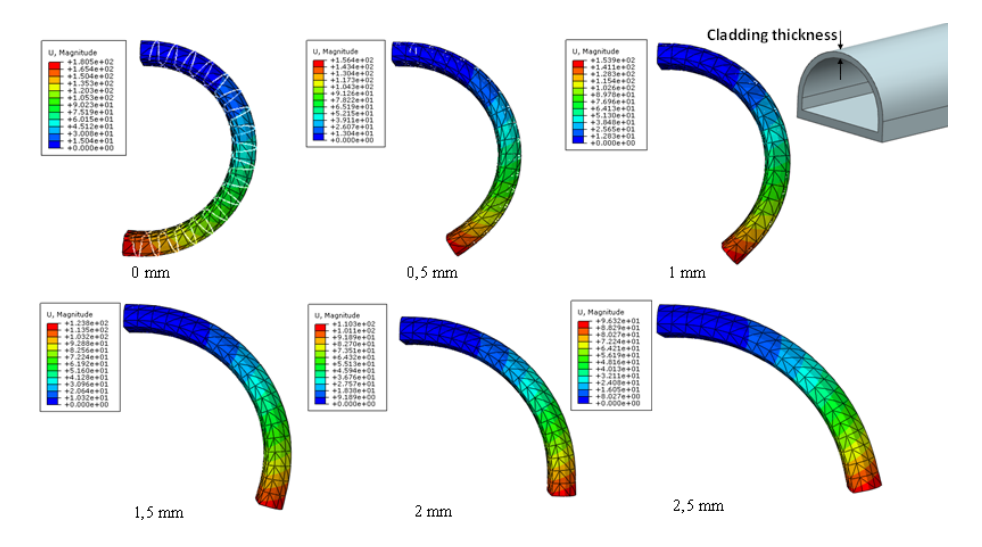


Fig. 6. The deformation of the composite soft actuator with the variable cladding layer thickness

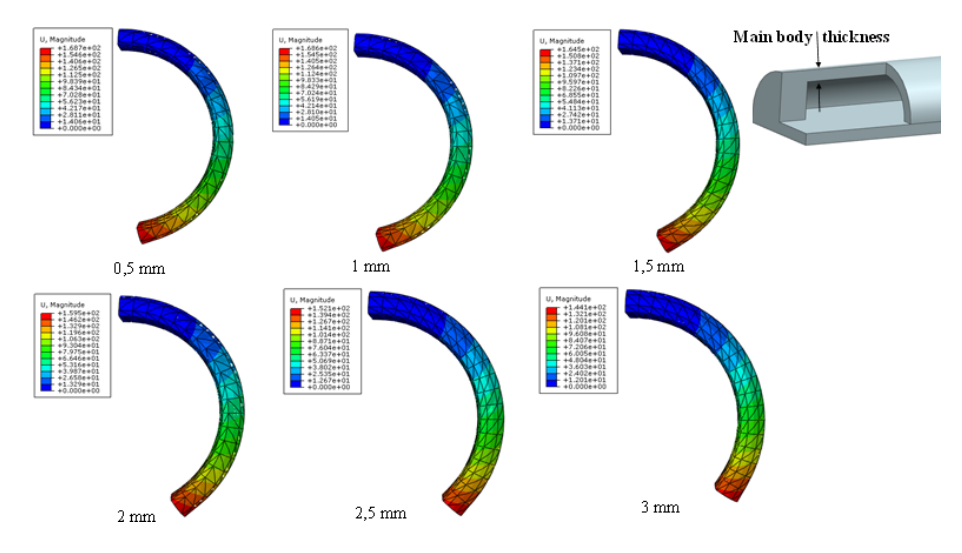


Fig. 7. The deformation of the composite soft actuator with the variable main body layer thickness

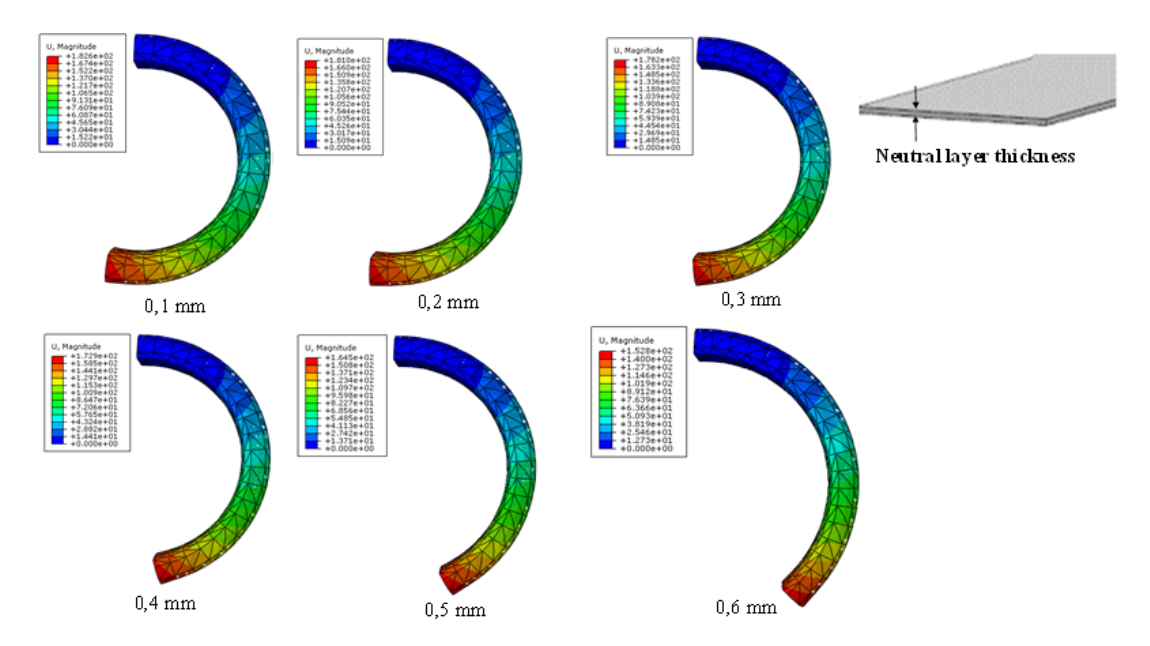


Fig. 8. The deformation of the composite soft actuator with the variable neutral layer thickness

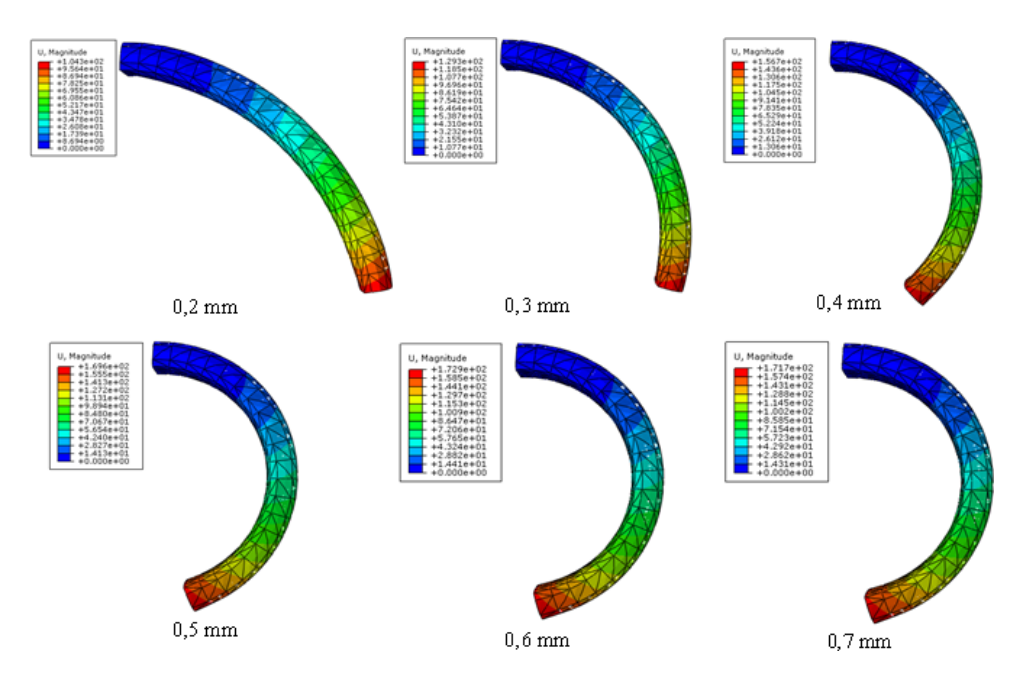


Fig. 9. The deformation of the composite soft actuator with the diameter of the reinforcement fiber

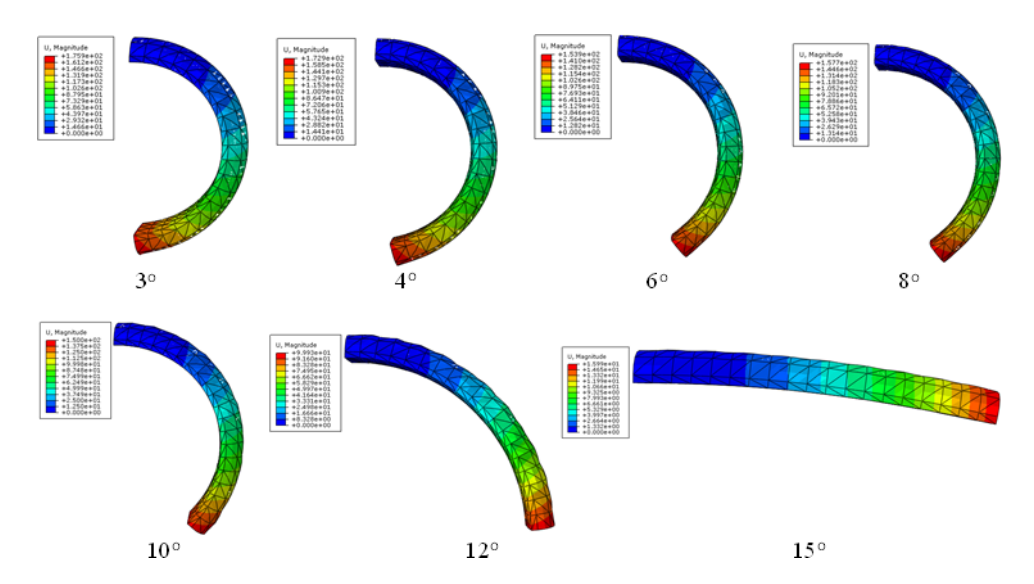


Fig. 10. The deformation of the composite soft actuator with the variable twist angle of the reinforcement fiber

Based on the numerical simulation results, the curvature of the composite soft actuator can be evaluated by measuring the bending angle (as shown in Fig. 11) under different values of pressures. The compared results of the above case studies are shown in Fig. 12 to Fig. 16.

The numerical simulation results depicted in Fig. 6 and Fig. 12 support the conclusion that an increase in the cladding thickness leads to a decrease in the bending angle of the actuator. Notably, a rapid decrease in the bending angle is observed for cladding thicknesses exceeding 1 mm. Therefore, it is recommended to use an optimal cladding thickness of 1 mm to achieve the desired actuator curvature while facilitating the fabrication process.

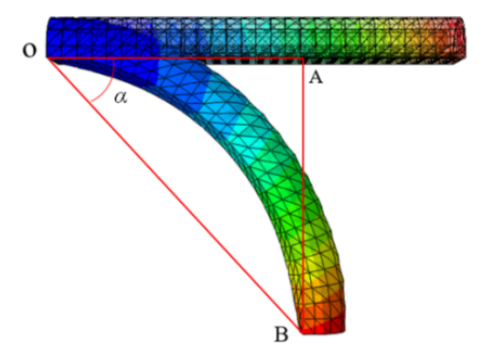
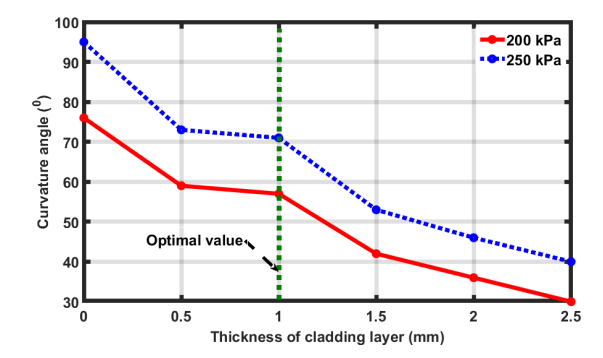
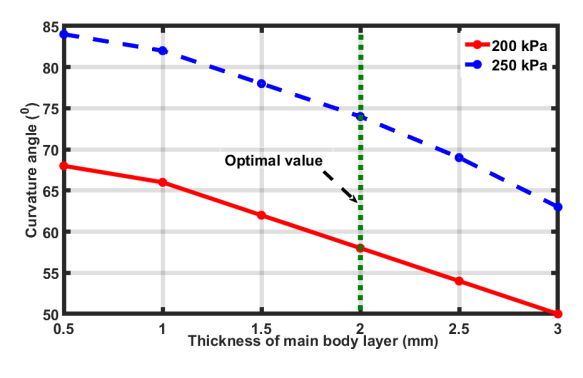


Fig. 11. The bending angle to evaluate the deformation of the composite soft actuator



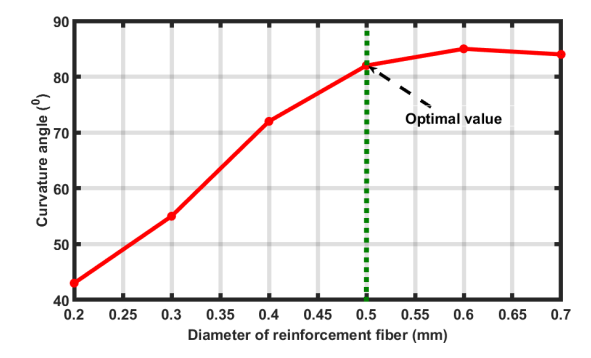
*Fig.* 12. The curvature angle with variable thickness of the cladding layer



Optimal value

*Fig.* 13. The curvature angle with variable thickness of the main body layer

Fig. 14. The curvature angle with variable thickness of the neutral layer



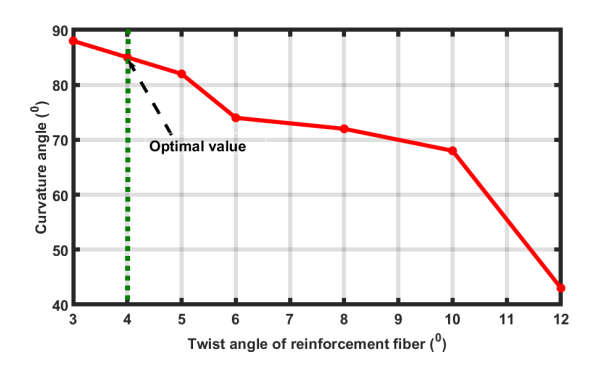


*Fig. 15.* The curvature angle with variable diameters of the reinforcement fiber

*Fig. 16.* The curvature angle with variable twist angles of the reinforcement fiber

Similarly, the results shown in Fig. 7 and Fig. 13 indicate that the bending angle of the soft finger gradually decreases as the thickness of the main body layer increases, aligning with the expected calculations. To achieve the optimal degree of curvature and manufacturing considerations, a recommended thickness of 2 mm is suggested for the main body layer.

Regarding the neutral layer thickness, the results from Fig. 8 and Fig. 14 demonstrate that an increase in the thickness leads to a decrease in the bending angle of the soft finger at the same pressure level. The optimal result is achieved with a neutral layer thickness of 0.1 mm. However, taking practical considerations into account, a neutral layer thickness of 0.2 mm may be chosen, as it provides a bending angle that is not significantly different from the case with a 0.1 mm neutral layer thickness.

The obtained results presented in Fig. 9 and Fig. 15 reveal that there exists an optimal wire cross-sectional diameter for achieving the desired bending angle of the actuator. Specifically, the best results are obtained with a wire diameter of 0.6 mm. However, it is worth noting that the bending angle does not change significantly when the wire

diameter is 0.5 mm compared to 0.6 mm. Hence, selecting a wire diameter of 0.5 mm may still yield satisfactory results while potentially reducing material and manufacturing costs.

Finally, the results depicted in Fig. 10 and Fig. 16 demonstrate that the bending angle of the soft actuator decreases as the helix angle of the reinforcement increases. Notably, when the twist angle exceeds  $10^{\circ}$ , a significant decrease in the bending angle is observed under the same applied pressure. However, when comparing the bending angles for twist angles of  $3^{\circ}$  and  $5^{\circ}$ , no significant difference is observed. Therefore, a suitable twist angle of  $4^{\circ}$  is recommended for the reinforcement to achieve the desired curvature.

The optimal values of these parameters are indicated with annotations in Figs. 12 to 16 and are summarized in Table 1 as follows.

Parameter	Optimal Value	Explanation
Cladding layer thickness	1 mm	Obtain desired curvature and facilitating fabrication
Main body layer thickness	2 mm	Achieves curvature efficiency and manufacturing considerations
Neutral layer thickness	0.2 mm	Obtain desired curvature
Reinforcement fiber diameter	0.5 mm	Provides optimal bending with reduced material cost
Reinforcement fiber twist angle	4°	Achieves desired curvature

Table 1. Optimal parameter values and their explanation

### 3. EXPERIMENTS

Based on the comprehensive investigation conducted in the aforementioned cases, the optimal design parameters for a composite soft actuator are as follows: The thickness of the cladding layer, main body layer, and neutral layer is 1 mm, 2 mm, and 0.2 mm, respectively. The fiber reinforcement layer features a wire diameter of 0.5 mm and a twist angle of  $4^{\circ}$ . These design parameters were utilized to fabricate the soft actuators for experimental purposes, thereby verifying the accuracy of the simulation results obtained through the Python-based automated calculation program implemented in Abaqus software. Furthermore, to achieve a more intricate curvature in the actuator, where each segment exhibits different radii of curvature, the design of the neutral layer was modified along the length of the actuator. The parameters of this design are illustrated in Fig. 17. Here,  $a_i$  represents the length of the neutral layers along the actuator,  $b_i$  denotes

the distance between adjacent neutral layers. These variables affect the curvature distribution of specific sections of the actuator. In the experimental setup, the corresponding values are as follows: l=140 mm,  $a_1=a_2=a_3=40$  mm, and  $b_1=5$  mm,  $b_2=15$  mm.

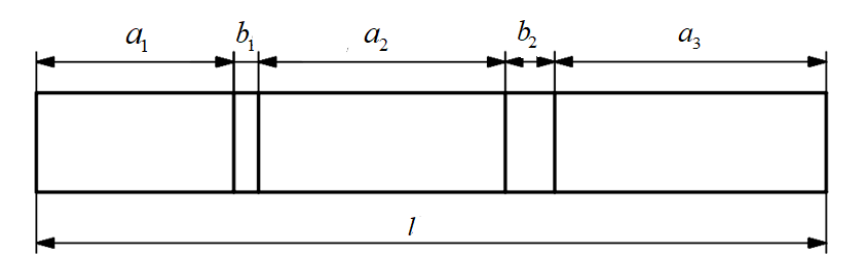


Fig. 17. The design of the neutral layer was modified along the length of the actuator



Fig. 18. The actuator after completion of the fabrication process

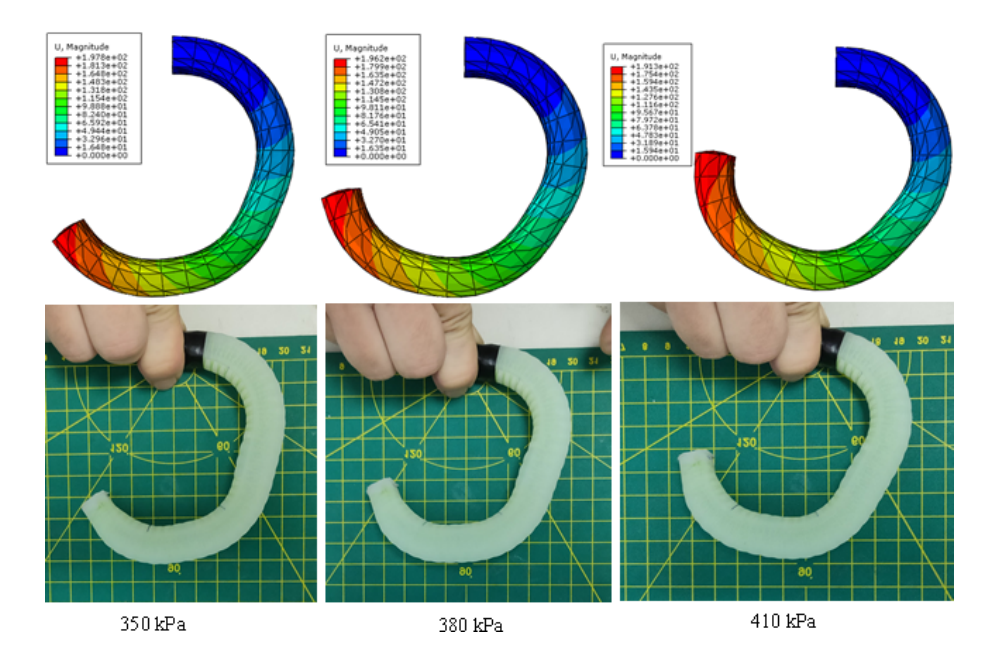


Fig. 19. The simulation and experiment results

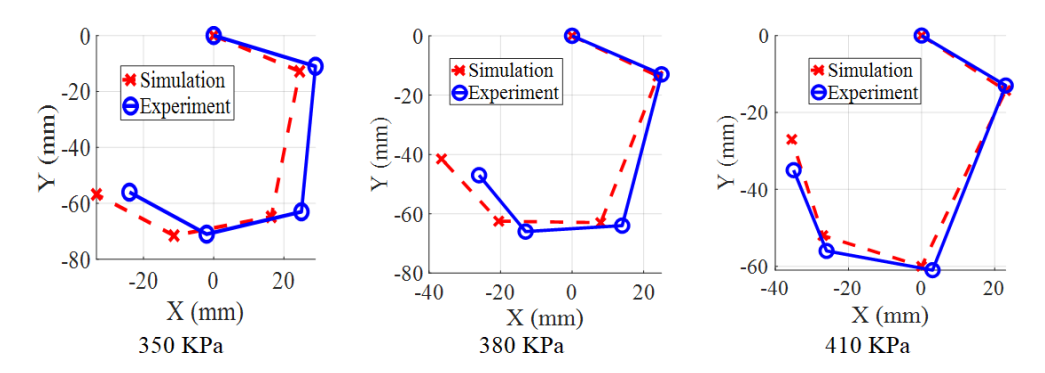


Fig. 20. The actuator's deformation is assessed across five segments

The fabrication process of the actuator follows a similar method as previously described in [25,28]. After completion of the fabrication process, the actuator is depicted in Fig. 18. The fabricated actuator is then used to experiment for measuring its deformation under varying pressure values. In the experiment setup, the compressed air pressure was controlled using a pressure gauge, and the actuator's curvature was estimated using a grid board, as depicted in Fig. 19. The results comparing the actuator's curvature at pressure values of 350 kPa, 380 kPa, and 410 kPa obtained from both simulation and experiment are presented in Fig. 20.

The obtained results demonstrate that the deformation simulation of the actuator when employing the calculation kernel of Abaqus in conjunction with the automated calculation program, yields accurate results while significantly reducing the computation time. To facilitate a more detailed comparison, the actuator's deformation is assessed across five segments, with the bending angle considered constant for each segment. The results in Fig. 20 indicate a relatively close agreement between the simulation and experimental data, with minimal differences observed. The largest error recorded is less than 10%.

## 4. CONCLUSIONS

Modeling deformation to optimize the design parameters of soft robotic structures, particularly composite soft actuators, is always a challenging task. Mathematical models often rely on numerous assumptions regarding material properties and geometric configurations, making them suitable only for specific structures. Meanwhile, traditional simulation approaches demand significant computational time and resources, particularly for complex structures like composite soft actuators, which makes them unsuitable for concurrent investigations of multiple design parameters. In this paper, we propose a technique to expedite the deformation simulation of composite soft actuators. We achieve this by utilizing a Python-based computational automation program integrated with the

computational kernel of Abaqus software. This program facilitates the automatic modification of input parameters while preserving properties, constraints, and boundary conditions that remain unchanged. Consequently, this approach significantly reduces the simulation time. Specifically, with the applied technique, the simulation time to modify an investigating parameter is approximately 10 minutes, whereas traditional simulations typically require around 60 minutes for the same task. The developed program is employed to analyze the impact of design parameters on the curvature of composite soft actuators, leading to the determination of optimal design parameters. Experimental verification demonstrates the reliability and efficiency of our technique. Comparison results reveal that the proposed approach yields deformation simulation results with less than a 10% error compared to measurements obtained from physical experiments. This confirms that the suggested approach is a viable solution to accelerate the simulation process, especially for soft robot structures. It enables swift investigation of the influence of design parameters, consequently facilitating the identification of optimal design structures tailored to specific objectives.

Although the numerical simulation has good results, with an error of less than 10%. However, the accuracy of this method can be improved with the following potential solutions. Firstly, using more advanced material models, such as Ogden or Gent, which can simulate the deformation of hyperelastic materials more accurately. These models require more complex experiments to determine the material parameters. Secondly, increasing the finite element mesh density, particularly in regions with large curvature deformation, needs to be conducted. Thirdly, a more detailed study of the nonlinear interactions in the contact between the reinforcement fiber and the main body layer is needed. These solutions will be explored in our future studies.

## **DECLARATION OF COMPETING INTEREST**

The authors declare that they have no known competing financial interests or personal relationships that could have appeared to influence the work reported in this paper.

### **FUNDING**

This research received no specific grant from any funding agency in the public, commercial, or not-for-profit sectors.

### REFERENCES

[1] B. Mazzolai, A. Mondini, E. Del Dottore, L. Margheri, F. Carpi, K. Suzumori, M. Cianchetti, T. Speck, S. K. Smoukov, I. Burgert, T. Keplinger, G. D. F. Siqueira, F. Vanneste, O. Goury, C. Duriez, T. Nanayakkara, B. Vanderborght, J. Brancart, S. Terryn, S. I. Rich, R. Liu,

- K. Fukuda, T. Someya, M. Calisti, C. Laschi, W. Sun, G. Wang, L. Wen, R. Baines, S. K. Patiballa, R. Kramer-Bottiglio, D. Rus, P. Fischer, F. C. Simmel, and A. Lendlein. Roadmap on soft robotics: multifunctionality, adaptability and growth without borders. *Multifunctional Materials*, 5, (2022). https://doi.org/10.1088/2399-7532/ac4c95.
- [2] O. Yasa, Y. Toshimitsu, M. Y. Michelis, L. S. Jones, M. Filippi, T. Buchner, and R. K. Katzschmann. An overview of soft robotics. *Annual Review of Control, Robotics, and Autonomous Systems*, **6**, (2023), pp. 1–29. https://doi.org/10.1146/annurev-control-062322-100607.
- [3] M. Li, A. Pal, A. Aghakhani, A. Pena-Francesch, and M. Sitti. Soft actuators for real-world applications. *Nature Reviews Materials*, 7, (2021), pp. 235–249. https://doi.org/10.1038/s41578-021-00389-7.
- [4] Y. Jiang, S. Yin, J. Dong, and O. Kaynak. A review on soft sensors for monitoring, control, and optimization of industrial processes. *IEEE Sensors Journal*, **21**, (2021), pp. 12868–12881. https://doi.org/10.1109/jsen.2020.3033153.
- [5] C. S. X. Ng, M. W. M. Tan, C. Xu, Z. Yang, P. S. Lee, and G. Z. Lum. Locomotion of miniature soft robots. *Advanced Materials*, 33, (2020). https://doi.org/10.1002/adma.202003558.
- [6] A. Zolfagharian, A. Z. Kouzani, S. Y. Khoo, A. A. A. Moghadam, I. Gibson, and A. Kaynak. Evolution of 3D printed soft actuators. *Sensors and Actuators A: Physical*, **250**, (2016), pp. 258–272. https://doi.org/10.1016/j.sna.2016.09.028.
- [7] Y. Chen, J. Yang, X. Zhang, Y. Feng, H. Zeng, L. Wang, and W. Feng. Light-driven bimorph soft actuators: design, fabrication, and properties. *Materials Horizons*, **8**, (3), (2021), pp. 728–757. https://doi.org/10.1039/d0mh01406k.
- [8] Y. Tang, M. Li, T. Wang, X. Dong, W. Hu, and M. Sitti. Wireless miniature magnetic phase-change soft actuators. *Advanced Materials*, **34**, (2022). https://doi.org/10.1002/adma.202204185.
- [9] M. Pan, C. Yuan, X. Liang, T. Dong, T. Liu, J. Zhang, J. Zou, H. Yang, and C. Bowen. Soft actuators and robotic devices for rehabilitation and assistance. *Advanced Intelligent Systems*, 4, (4), (2022). https://doi.org/10.1002/aisy.202100140.
- [10] H. Al-Fahaam, S. Davis, and S. Nefti-Meziani. Power assistive and rehabilitation wearable robot based on pneumatic soft actuators. In 2016 21st International Conference on Methods and Models in Automation and Robotics (MMAR), IEEE, (2016), pp. 472–477. https://doi.org/10.1109/mmar.2016.7575181.
- [11] S. Chen, Y. Pang, H. Yuan, X. Tan, and C. Cao. Smart soft actuators and grippers enabled by self-powered tribo-skins. *Advanced Materials Technologies*, **5**, (2020). https://doi.org/10.1002/admt.201901075.
- [12] H. Rodrigue, W. Wang, D.-R. Kim, and S.-H. Ahn. Curved shape memory alloy-based soft actuators and application to soft gripper. *Composite Structures*, **176**, (2017), pp. 398–406. https://doi.org/10.1016/j.compstruct.2017.05.056.
- [13] H. Su, X. Hou, X. Zhang, W. Qi, S. Cai, X. Xiong, and J. Guo. Pneumatic soft robots: challenges and benefits. *Actuators*, 11, (2022). https://doi.org/10.3390/act11030092.
- [14] Q. Xie, T. Wang, S. Yao, Z. Zhu, N. Tan, and S. Zhu. Design and modeling of a hydraulic soft actuator with three degrees of freedom. *Smart Materials and Structures*, **29**, (2020). https://doi.org/10.1088/1361-665x/abc26e.
- [15] B. W. K. Ang and C.-H. Yeow. Design and modeling of a high force soft actuator for assisted elbow flexion. *IEEE Robotics and Automation Letters*, **5**, (2020), pp. 3731–3736. https://doi.org/10.1109/lra.2020.2980990.

- [16] G. Chen, X. Yang, X. Zhang, and H. Hu. Water hydraulic soft actuators for underwater autonomous robotic systems. *Applied Ocean Research*, **109**, (2021). https://doi.org/10.1016/j.apor.2021.102551.
- [17] A. Miriyev, K. Stack, and H. Lipson. Soft material for soft actuators. *Nature Communications*, **8**, (2017). https://doi.org/10.1038/s41467-017-00685-3.
- [18] J. Hu, M. Yu, M. Wang, K.-L. Choy, and H. Yu. Design, regulation, and applications of soft actuators based on liquid-crystalline polymers and their composites. *ACS Applied Materials & Interfaces*, **14**, (2022), pp. 12951–12963. https://doi.org/10.1021/acsami.1c25103.
- [19] A. Miriyev, B. Xia, J. C. Joseph, and H. Lipson. Additive manufacturing of silicone composites for soft actuation. *3D Printing and Additive Manufacturing*, **6**, (2019), pp. 309–318. https://doi.org/10.1089/3dp.2019.0116.
- [20] P. Polygerinos, Z. Wang, J. T. B. Overvelde, K. C. Galloway, R. J. Wood, K. Bertoldi, and C. J. Walsh. Modeling of soft fiber-reinforced bending actuators. *IEEE Transactions on Robotics*, **31**, (2015), pp. 778–789. https://doi.org/10.1109/tro.2015.2428504.
- [21] S. Nikolov, V. Kotev, K. Kostadinov, F. Wang, C. Liang, and Y. Tian. Model-based design optimization of soft fiber-reinforced bending actuators. In 2016 IEEE International Conference on Manipulation, Manufacturing and Measurement on the Nanoscale (3M-NANO), IEEE, (2016), pp. 136–140. https://doi.org/10.1109/3m-nano.2016.7824949.
- [22] M. H. Namdar Ghalati, H. Ghafarirad, A. A. Suratgar, M. Zareinejad, and M. A. Ahmadi-Pajouh. Static modeling of soft reinforced bending actuator considering external force constraints. *Soft Robotics*, **9**, (2022), pp. 776–787. https://doi.org/10.1089/soro.2021.0010.
- [23] F. Connolly, P. Polygerinos, C. J. Walsh, and K. Bertoldi. Mechanical programming of soft actuators by varying fiber angle. *Soft Robotics*, **2**, (2015), pp. 26–32. https://doi.org/10.1089/soro.2015.0001.
- [24] Z. Wang, P. Polygerinos, J. T. B. Overvelde, K. C. Galloway, K. Bertoldi, and C. J. Walsh. Interaction forces of soft fiber reinforced bending actuators. *IEEE/ASME Transactions on Mechatronics*, **22**, (2017), pp. 717–727. https://doi.org/10.1109/tmech.2016.2638468.
- [25] P. Polygerinos, Z. Wang, K. C. Galloway, R. J. Wood, and C. J. Walsh. Soft robotic glove for combined assistance and at-home rehabilitation. *Robotics and Autonomous Systems*, **73**, (2015), pp. 135–143. https://doi.org/10.1016/j.robot.2014.08.014.
- [26] L. Gharavi, M. Zareinejad, and A. Ohadi. Continuum analysis of a soft bending actuator dynamics. *Mechatronics*, **83**, (2022). https://doi.org/10.1016/j.mechatronics.2022.102739.
- [27] S. K. Melly, L. Liu, Y. Liu, and J. Leng. A review on material models for isotropic hyperelasticity. *International Journal of Mechanical System Dynamics*, **1**, (2021), pp. 71–88. https://doi.org/10.1002/msd2.12013.
- [28] H. X. Trinh, P. V. Binh, L. D. Manh, N. V. Manh, and N. V. Quang. Soft robotics-fingered hand based on working principle of asymmetric soft actuator. In *Machine Learning and Mechanics Based Soft Computing Applications*, Springer Nature Singapore, (2023), pp. 89–95. https://doi.org/10.1007/978-981-19-6450-3\_10.